

Reducing Visual Confusion with Discriminative Attention

Lezi Wang, Ziyang Wu, Srikrishna Karanam, Kuan-Chuan Peng, and Rajat Vikram Singh
Siemens Corporate Technology, Princeton, NJ
{first.last, singh.rajat}@siemens.com

Abstract

Recent developments in gradient-based attention modeling have led to improved model interpretability by means of class-specific attention maps. A key limitation, however, of these approaches is that the resulting attention maps, while being well localized, are not class discriminative. In this paper, we address this limitation with a new learning framework that makes class-discriminative attention and cross-layer attention consistency a principled and explicit part of the learning process. Furthermore, our framework provides attention guidance to the model in an end-to-end fashion, resulting in better discriminability and reduced visual confusion. We conduct extensive experiments on various image classification benchmarks with our proposed framework and demonstrate its efficacy by means of improved classification accuracy including CIFAR-100 (+3.46%), Caltech-256 (+1.64%), ImageNet (+0.92%), CUB-200-2011 (+4.8%) and PASCAL VOC2012 (+5.78%).

1. Introduction

Image classification has seen tremendous progress in the last few years, driven by recent advances in convolutional neural networks (CNNs) [11, 15]. Understanding why CNNs make the predictions they do can help make models interpretable as well as provide cues to design improved algorithms.

In recent years, network attention has emerged as a powerful tool for interpreting CNNs [4, 25, 39], providing ways to generate category-specific attention maps. The big-picture intuition that drives these techniques is to answer the following question- *where is the target object in the image?*. Some recent extensions [17] make attention end-to-end trainable, producing attention maps that provide improved answers to the localization question above. While these methods consider the localization problem, this is not sufficient for image classification, where the model needs to be able to tell various object categories apart. Specifically, these methods produce attention maps specific to each class of interest, whereas for image classification, we

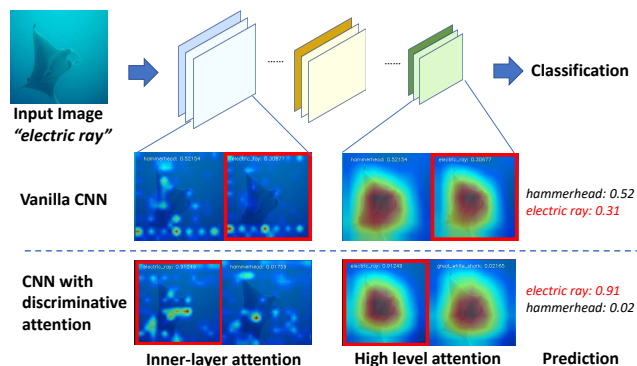


Figure 1. Discriminative attention leads to better model interpretability, as well as improved classification accuracy. Discriminative attention modeling can be incorporated at different layers in a CNN. In the top layers, the model attends to the similar regions while it can find discriminative patterns in lower inner layers for confusing categories.

want these attention maps to be *discriminative* across categories as well. Our intuition, illustrated in Figure 1, is that such separable attention maps can lead to better model interpretability for classification, and better yet, improved classification performance. Furthermore, we contend that false classifications stem from patterns across categories that confuse the model, and that eliminating these confusing patterns can lead to better model generalizability. To illustrate this better, consider Figure 2, where we use the trained VGG-19 model [27] to perform classification on the ILSVRC2012 [24] dataset, collect failure cases and generate the attention maps via Grad-CAM [25], showing the top-5 predictions. As can be seen from the figure, while the attention maps are well localized, there are large overlapping regions between the target category’s attention (marked by red bounding box) maps and those of the false positives, demonstrating the problem of attention discriminability.

With the considerations discussed above, we ask two key questions: (a) can we make category-specific attention maps separable and discriminative across different categories, thereby reducing visual confusion?, and (b) can

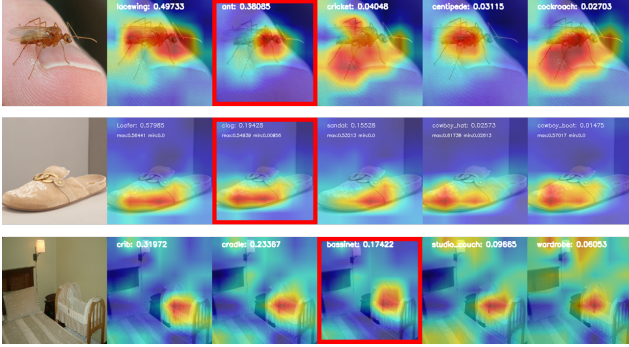


Figure 2. Model attention maps for the top-5 predictions. Attention maps are generated by Grad-CAM and the prediction with red-bounding boxes correspond to the target category. All the target classes are not ranked as top-1 and their activation maps have large overlap with false positives (top-1 prediction).

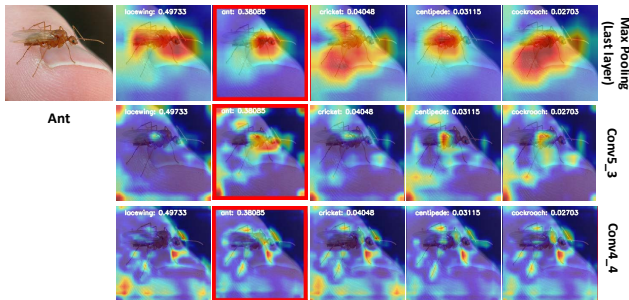


Figure 3. Models attention maps from different feature layers. Attention maps are generated from Grad-CAM [25], and those of different categories from intermediate layers (Conv5_3, Conv4_4) have less overlap than the last layer (top row).

we incorporate attention discriminability in the learning process in an end-to-end fashion? In this paper, we answer these questions in a principled manner, proposing the first framework that makes attention maps class discriminative. Furthermore, we propose a new mechanism to guide our model towards attention discriminability, providing for end-to-end supervisory signals by explicitly constraining attention maps of various categories to be separable.

As discussed above, attention separability and discriminability is a key aspect of our proposed learning framework. Figure 2 showed us that while attention maps from the last layer are reasonably complete, they are not separable. This prompted us to look “further inside” the CNN, with Figure 3 showing attention maps from several intermediate layers of the network. It is reasonably clear from the illustration that attention maps from these inner layers are more separable than those from the last layer. However, some problems still exist- the inner layer attention maps are not as complete or localized as those from the last layer. So, the question we ask is- can we get the separability of the inner layer attention and the localization of the last layer attention at the same time? This would result in a “best-

of-both-worlds” attention map that is both separable and complete, which is what we set out to achieve. To this end, our framework also includes an explicit mechanism that enforces attention consistency among attention maps of the target categories. We conduct extensive experiments on five highly competitive benchmark datasets (CIFAR-100 [16], Caltech-256 [10], ILSVRC2012 [24], CUB-200-2011 [30] and PASCAL VOC 2012 [8]), demonstrating performance improvements of 3.46%, 1.64%, 0.92%, 4.8%, and 5.78% respectively.

To summarize, the key contributions of the paper include:

- We present the first learning objective to enforce the model to produce category-discriminative attention maps, resulting in improved attention separability.
- We present the first learning objective to enforce attention consistency across different layers, resulting in improved localization with “inner-layer” attention maps.
- We present the first framework that integrates category-discriminative attention and cross-layer attention consistency in a common learning framework, providing the model with a principled learning objective to produce discriminative and consistent attention maps across various categories.

2. Related work

Visualizing CNNs. Much recent effort has been expended in visualizing internal representations of CNNs to better understand and interpret the model. In [26, 28, 35], the gradient of the prediction is computed w.r.t. the specific CNN unit, *i.e.* the input image, to highlight important pixels. Specifically, Simonyan *et al.* [26] visualized partial derivatives of predicted class scores w.r.t. pixel intensities, whereas guided backpropagation [28] and deconvolution [35] modified “raw” gradients to result in better visualization. Despite producing fine-grained visualizations, these methods are not class discriminative.

Erhan *et al.* [7] synthesize the images to maximally activate a network unit. Mahendran *et al.* [19] and Dosovitskiy *et al.* [6] analyze the visual coding to invert latent representation. They perform image reconstruction by inverting the features with an up-convolutional neural network.

Our framework is inspired by recent works [4, 25, 39] addressing category-specific attention maps. CAM [39] generated the class activation maps highlighting the task relevant region by replacing fully-connected layers with convolution and global average pooling. A drawback of CAM is inflexibility, requiring retraining of classifiers and feature maps to directly precede softmax layers, hindering its applicability to any feature layers. Grad-CAM [25] was

proposed to address these issue, where without retraining and changing the network architecture, class activation maps were generated by weighted combination of feature maps in various channels. The weights were computed by averaging the gradient of the final prediction w.r.t. the pixels in the feature map. However, we observe that such simple averaging is unable to measure channel importance properly, resulting in substantial attention inconsistency among various feature layers. While Grad-CAM++ [4] proposed a better class activation map by modifying the way weights are computed, its high computational cost in calculating the second and third derivatives makes it impractical to be used during model training.

Attention-guided network training.

Several recent methods [12, 15, 32, 34] have attempted to incorporate attention processing to improve the performance of CNNs in large-scale image classification. Wang *et al.* [32] proposed Residual Attention Network, modifying the Residual Network (ResNet) [11] by adding the hourglass network [20] to the skip-connection to generate attention masks, which are then used to refine feature maps. Hu *et al.* [12] introduced a Squeeze-and-Excitation module which uses the globally average-pooled features to compute channel-wise attention. CBAM [21, 34] modified the Squeeze-and-Excitation module to exploit both spatial and channel-wise attention. Closer to our work, Jetley *et al.* [15] estimated attention by taking feature maps at various layers in the CNN as input, producing a 2D matrix of scores for each map. The ensemble of output scores were then used for category prediction. While these methods use attention for downstream classification, they do not explicitly use category-specific attention as part of training a model towards the image classification objective. Our work, to the best of our knowledge, is the first to make category-specific attention end-to-end trainable with the specific goal of guiding the model with attention separability and cross-layer attention consistency as supervisory signals. Furthermore, our proposed method can be considered as an add-on module to existing image classification architectures without needing any architectural change, unlike other methods [12, 15, 32, 34].

Category-specific attention has been used in the past for weakly-supervised object localization and semantic segmentation tasks [5, 17, 33, 37]. The intuition here was that given only image-level annotations, attention from the last feature layer can be used to improve spatial localization of the target category. Compared to these methods, we model attention differently. While the goal of these methods is singular, *i.e.*, good target localization, our goal is two-fold, good target localization as well as discriminability from other categories. To this end, we devise novel objective functions to guide our model towards discriminative attention across different categories, leading to improved

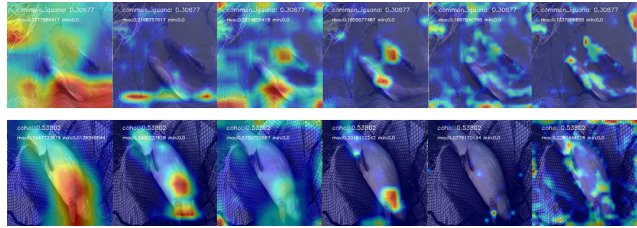


Figure 4. Attentions maps computed with Grad-CAM from different feature layers for two categories(top and bottom). For each category, attention maps from higher to lower layers are listed left to right. For the same category, we see model attention shift across the layers.

classification performance as we demonstrate later.

3. Approach

We present an end-to-end learning framework to improve model generalizability and interpretability for image classification by means of attention-guided training. The general idea is to produce separable attention, across various categories, that will then provide supervisory signals for the model trained towards the classification objective. To this end, we propose a new differentiable intersection-over-union learning objective to enforce such attention discriminability. Our observations, discussed previously, suggest that attention maps computed with existing methods such as Grad-CAM [25] do not produce category-separable attention from the last layer, although they are reasonably well localized. Consequently, we look deeper inside the network, noticing that inner layer attention has the potential to be separable. This suggests we consider both inner layer and last layer attention to get separability and localization. To this end, we propose a new cross-layer attention consistency learning objective to enforce consistency in inner and last layer attention. Both our proposed learning objectives require that we obtain reasonable attention maps from the inner layer. However, Grad-CAM [25], while showing promise in generating separable attention, fails to produce intuitively satisfying attention maps from the inner layer. To illustrate this better, we depict the Grad-CAM of two categories in Figure 4. As we can see from this figure, we need better inner layer attention that we can use in our learning framework- to this end, we first propose a new mechanism to generate improved attention maps. We then proceed to discussing how we use the improved attention maps to produce principled supervisory signals for attention separability and cross-layer consistency.

3.1. Improved attention generation

We first begin by describing our improved method to compute gradient-based attention. Three commonly used techniques exist to compute gradient-based attention maps

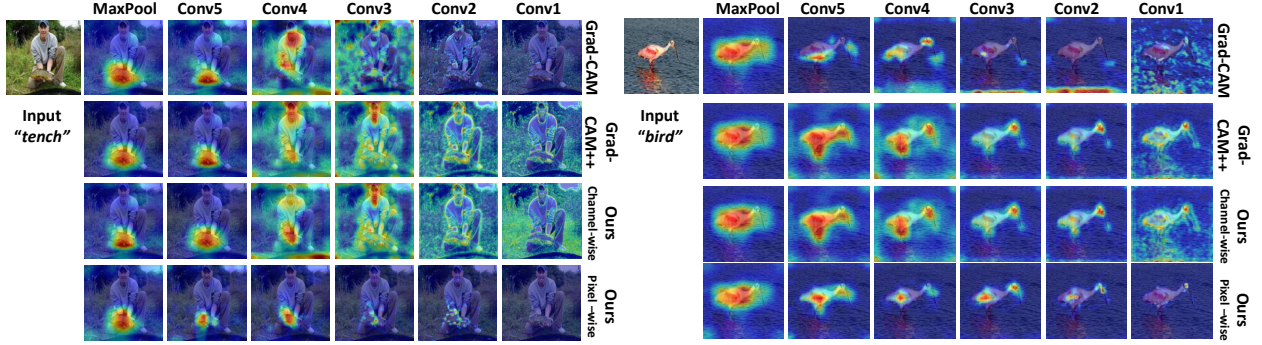


Figure 5. A comparison of four types of attention maps. Our pixel-wise attention shows the best cross-layer consistency in that the model attends to the target object across all the layers. Our channel-wise attention has the similar visual explanation to the Grad-CAM++.

given category labels- CAM [39], Grad-CAM [25], and Grad-CAM++ [4]. We do not use CAM because (a) it is inflexible, requiring architecture modification for generating trainable attention and (b) works only for the last feature layer. Although Grad-CAM and Grad-CAM++ are more flexible and can be used to generate inner layer attention, they have several drawbacks we address next.

Grad-CAM [25] and Grad-CAM++ [4] are both flexible when compared to CAM [39] in the sense that they only need to compute the gradient of the class prediction w.r.t. feature maps to measure the importance of each feature map pixel. Specifically, the class-specific gradient Y^c is determined by computing $(\partial Y^c)/(\partial F^k)$, where F^k is the feature map using which the attention is computed. Categorical attention maps are then generated as \mathcal{A} :

$$\mathcal{A} = ReLU\left(\sum_k \alpha_k^c F^k\right), \quad (1)$$

where α_k^c indicates the importance of the feature map F^k in the k -th channel. In Grad-CAM [25], the weight α_k^c is a global average of the pixel importance in $(\partial Y^c)/(\partial F^k)$:

$$\alpha_k^c = \frac{1}{Z} \sum_i \sum_j \frac{\partial Y^c}{\partial F_{ij}^k} \quad (2)$$

Grad-CAM++ [4] uses higher order derivatives (second and third) to compute the channel weights, leading to better visual explanations at increased computational cost.

There are three key drawbacks with Grad-CAM and Grad-CAM++ [4, 25] that hinder their use *as is* for our purposes of providing separable and consistent attention guidance towards the image classification objective. First, there are large attention shifts among attention maps from different network layers in Grad-CAM [25] which are caused by negative gradients while computing channel-wise importance. Recall that a key aspect of our framework is to use the separability that we observe in inner layer attention in addition to the good localization from the last layer attention. While we observe relatively less attention shift with

Method	Top-1 Acc.	Δ
ResNet-110 + $\mathcal{A}_{Grad-CAM}$	74.02	-
ResNet-110 + \mathcal{A}_{px}	76.24	2.22
ResNet-110 + \mathcal{A}_{ch}	76.11	2.09

Table 1. The results of generic image classification on CIFAR-100. The last column Δ indicates performance improvement of the network with our attention-driven supervision when compared to the baseline model.

Grad-CAM++ [4], the high computational costs involved in computing higher order derivatives precludes its use in our framework since we wish to use attention maps from multiple layers to guide model training.

To address the issues discussed above, we propose two kinds of category-specific attention computation mechanisms, modeling channel- and pixel-wise attention. Our channel-wise attention has similar visual explanations as Grad-CAM++, as shown in Figure 5, without needing to compute the higher order derivatives as in Grad-CAM++, resulting in more complete attention maps with relatively less attention shift unlike GradCAM. Our pixel-wise attention produces attention maps focused on the sharp, high-frequency regions, bringing out fine details, while having a low computational cost as Grad-CAM.

Channel-wise attention Our observation is that the inconsistency noted above among attention maps from different network layers with GradCAM is due to negative gradients from background pixels. In Grad-CAM, all pixels of the gradient map contribute equally to the channel weight, as can be noted from Eq. 2. Due to this reason, in cases where background regions dominate, the model tends to attend only to small regions of target objects, ignoring other regions that are important for category discrimination.

We are motivated by observations in related interpretability work [4, 28, 35] that note that positive gradients w.r.t. each pixel in an activation map strongly correlate with the importance of the activation map for a certain category. A positive gradient at specific location implies increasing

the pixel intensity would have positive impact on the prediction score Y^c . To this end, we propose a new mechanism, driven by positive gradients, to compute the channel importance α_k^c of a particular activation map F^k :

$$\alpha_k^c = \frac{1}{Z} \sum_i \sum_j ReLU\left(\frac{\partial Y^c}{\partial F_{ij}^k}\right) \quad (3)$$

With our proposed channel importance score, our category-specific attention map computation mechanism is now defined as:

$$A_{ch} = \frac{1}{Z} ReLU\left(\sum_k \sum_i \sum_j ReLU\left(\frac{\partial Y^c}{\partial F_{ij}^k}\right) F^k\right) \quad (4)$$

Pixel-wise attention Our proposed attention generation mechanism above, as well as competing methods [4, 25, 39] are computed channel-wise, where pixels within the same channel share the same weight for feature map combination. However, as shown in Figure 5, we observe that computing attention in a pixel-wise produces attention maps that have better cross-layer consistency, as well as producing sharper high-frequency attentive regions. Such attention maps can help better visualize and understand the reasoning behind our model’s predictions. Specifically, each feature map F^k votes on the importance of the pixel at location (i, j) for predicting the target category c . In the feature map F^k , the pixel intensity is scaled by its importance measured as $(\partial Y^c)/(\partial F_{ij}^k)$, which is followed by an averaging operation across channels to obtain the pixel-wise attention as:

$$A_{px} = ReLU\left(\frac{1}{K} \sum_k \left\langle \frac{\partial Y^c}{\partial F^k}, F^k \right\rangle\right), \quad (5)$$

where the $\left\langle \frac{\partial Y^c}{\partial F^k}, F^k \right\rangle$ indicates element-wise multiplication of the gradient and feature maps.

3.2. Attention discrimination for reduced visual confusion

Our general intuition is that making category-specific attention maps separable will lead to better model generalizability and interpretability for image classification. Furthermore, we use this notion of attention separability as a principled part of our learning process, leading to an improved model trained towards the classification objective. To achieve this goal, we propose a new differentiable intersection-over-union (IoU) learning objective. Essentially, we enforce attention to be discriminative across categories, and we reflect this in the learning objective by means of quantifying overlapping regions in attention maps between the target category and the most confusing category. We next describe our proposed differentiable IoU objective.

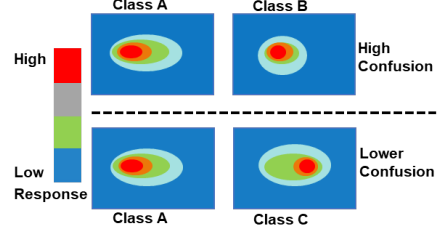


Figure 6. The differentiable soft intersection-over-union. According to the attention maps of class A, B and C, there is higher visual confusion between (A,B) than (A,C) due to high attention response at the same location.

3.2.1 Differentiable intersection-over-union for reduced attention overlap

Given the attention map of a target category \mathcal{A}^T and its most confusing category \mathcal{A}^{Conf} , we measure their attention overlap by computing the intersection over union (IoU). However, the traditional IoU is computed on maps with binary values, and is not differentiable. To this end, we propose a differentiable version, called soft IoU (sIoU) to measure the visual confusion among attention maps with real values:

$$sIoU = 2 \frac{\sum_{ij} (\min(\mathcal{A}_{ij}^T, \mathcal{A}_{ij}^{Conf}) \cdot Mask_{ij})}{\sum_{ij} (\mathcal{A}_{ij}^T + \mathcal{A}_{ij}^{Conf})}, \quad (6)$$

where the \cdot operator indicates the scalar product, and \mathcal{A}_{ij}^T and \mathcal{A}_{ij}^{Conf} represent the $(i, j)^{th}$ pixel in attention map \mathcal{A}^T and \mathcal{A}^{Conf} respectively.

The intuition of sIoU is illustrated in Figure 6. If the model attends to the same or overlapped regions for different categories, this results in visual confusion. We penalize this by reducing this overlap by means of the proposed sIoU objective, which is differentiable with value range from 0 to 1. By minimizing the sIoU, we explicitly reduce the overlap between the attention map of the target category and that of the most confusing category, leading to reduced confusion.

Additionally, to reduce noise from background pixels, we apply a mask to focus on pixels within the target object region for the sIoU computation. In Eq. 6, the $Mask$ indicates the target object region, generated via thresholding the attention map from the last layer \mathcal{A}^{last} :

$$Mask_{ij} = \frac{1}{1 + \exp(-\omega(\mathcal{A}_{ij}^{last} - \sigma))}, \quad (7)$$

where we empirically choose values of σ and ω to be $0.55 \cdot \max(\mathcal{A}_{ij}^{last})$ and 100 respectively.

The proposed sIoU can be considered an add-on module for training a model without changing the network architecture. Besides applying the sIoU to the last feature layer,

we can also compute the sIoU for any other layers, which makes it possible for us to check and modify the model’s attention in different scales.

While the proposed sIOU objective helps enforce attention separability, it is not sufficient for image classification since inner layer attention maps are not as spatially complete as the last layer ones. We set out to achieve an attention map that is both complete and category-discriminative, and to this end, we propose a new cross-layer attention consistency objective that enforces the target attention map from an inner layer feature map to be similar to that from the last layer. We next describe the constraints we enforce to this end.

3.3. Cross-layer attention consistency

In the higher layer, the model attention captures more semantic information, covering most of the target object [4, 25, 39]. For the intermediate layers with small receptive field of the convolution kernels, the CNN model attends to more fine-grained patterns as shown in Figure 5. Compared to the attention from higher layers, the attention of lower layer contains more noise, highlighting the background pixels. Additionally, direct minimizing the masked sIoU may lead to the trivial solution that the model attentions within target region converges to the low responses.

To address the above problems, we propose the attention consistency loss L_{ac} to rectify the model attention so that the highlighted fine-grained attention would be mainly localized in the target region:

$$L_{ac} = \alpha - \frac{\sum_{ij} (\mathcal{A}_{ij}^{in} \cdot Mask_{ij})}{\sum_{ij} \mathcal{A}_{ij}^{in}}, \quad (8)$$

where the \mathcal{A}^{in} indicates the attention maps from the intermediate feature layers. The purpose of loss L_{ac} is to maintain the intra-class consistency among different feature layers.

3.4. Overall training objective

To guide our model towards end-to-end learning via attention separability and cross-layer consistency as supervisory signals, we apply the constraints discussed above jointly. Specifically, as shown in Figure 7, we use the last convolutional layer in the penultimate block of ResNet to compute the inner layer attention map, which is used to enforce the soft IoU constraint for the inner layer $sIoU_i$. We also apply the soft IoU constraint on the attention map from the last layer, giving us the constraint $sIoU_l$. Finally, we apply the cross-layer consistency constraint L_{ac} between the attention maps from these two layers. In the experiment, for the classification loss L_{cls} , we use cross-entropy and multilabel-soft-margin loss for single and multi-label image classification respectively. Our overall training objective is given as:

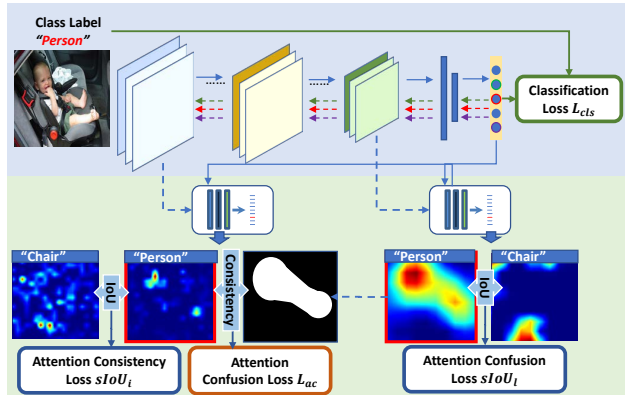


Figure 7. The training framework. Besides classification loss L_{cls} , the model is supervised by the soft IoU constraints of the last layer $sIoU_l$ and inter layer $sIoU_i$, and the attention consistency loss L_{ac} .

$$L = L_{cls} + sIoU_i + sIoU_l + L_{ac} \quad (9)$$

4. Experiments

We empirically demonstrate the efficacy of our proposed approach on several benchmark datasets and compare with the corresponding baseline model (with the same architecture) without our attention-drive supervision mechanism. Our experiments contain three parts for various image classification tasks. First, we evaluate our framework for generic image classification on three datasets: CIFAR-100 [16], Caltech-256 [10] and ILSVRC2012 [24]. Second, we apply our approach to fine-grained image classification on the CUB-200-2011 [30] dataset. Third, since our proposed framework is class-discriminative and is able to provide supervision for multi-label image classification, we also evaluate on the PASCAL VOC 2012 [8] dataset.

We perform the experiments using PyTorch [22] and NVIDIA Titan X GPUs. We do not search in the hyperparameter space for the best hyperparameters and instead use the same training parameters as those in the baseline proposed by the authors of corresponding papers.

4.1. Generic image classification

CIFAR-100: ResNet [11] is used as the baseline method. To conduct a fair comparison, we use similar experimental settings as in [11]. The image is padded by 4 pixels on each side, filled with 0 value resulting in a 40×40 image. A 32×32 crop is randomly sampled from an image or its horizontal flip, with the per-pixel RGB mean value subtracted. We adopt the same weight initialization method following [11] and train the ResNet using Stochastic Gradient Descent (SGD) [2] with a mini-batch size of 128. We use a weight decay of 0.0005 with a momentum of 0.9 and set the initial

learning rate to 0.1. The learning rate is divided by 10 at 81 and 122 epochs. The training is terminated after 160 epochs.

Caltech-256: There is no official train/test data split. We follow the work in [10] to randomly select 25 images per category as the testing set and 30, 60 images per category as training. We remove the last (257-th) category ‘clutter’, keeping the 256 categories which describe the specific objects. We use Vgg19 [26] and ResNet-18 [11] as the baseline models. For both the baseline and our proposed method’s training, we use a weight decay of 0.001 with a momentum of 0.9 and set the initial learning rate to 0.01. To speed up the model training, we adopt cyclic cosine annealing [13] with a cycle of one to train the network for 20 epochs .

ImageNet: We conduct large-scale image classification experiments using ImageNet LSVRC2012 dataset [24]. The evaluation is conducted on the images of the LSVRC2012 validation set. We use ResNet-18 [11] as the baseline model. We use SGD [2] with a mini-batch size of 256 to train the network. The initial learning rate is set as 0.1 and weight decay of 0.0001 with a momentum of 0.9. The learning rate is divided by 10 at 30 and 60 epochs. The training is terminated after 90 epochs.

Accuracy. Tables 2-4 show that the model trained with our proposed supervisory principles outperform the corresponding baseline models with a notable margin. The most noticeable performance improvements may be observed with the CIFAR-100 dataset in Table 2, which shows that, without changing the network architecture, the top-1 accuracy of ResNet-110 with supervision from \mathcal{A}_{px} and \mathcal{A}_{ch} exceeds the original model by a margin of 3.46% and 3.24% respectively. The supervised ResNet-110 also demonstrates superior performance over the one with stochastic depth and even the deeper model having 164 layers. As for the comparison between pixel and channel wise attention, pixel-wise attention \mathcal{A}_{px} , which provides the sharper high-frequency attentive regions, is better in capturing discriminative parts in low resolution images when compared to \mathcal{A}_{ch} . As can be observed from the qualitative results in Figure 8, our approach equips the model with discriminative attention among different categories, resulting in improved prediction. For the high-resolution images in Caltech-256 and ILSVR2012 datasets, the model supervised by the \mathcal{A}_{px} and \mathcal{A}_{ch} demonstrates $\sim 1\%$ performance improvement over baseline VGG-19 and ResNet-18 models.

4.2. Fine-grained Image Recognition

We evaluate our approach on CUB-2011 [31] dataset for fine-grained image recognition. The CUB-2011 contains 11,788 images of 200 species of birds with 5,994 images for training and 5,794 for testing. We follow the training

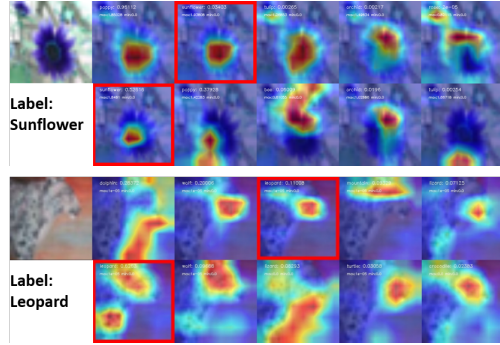


Figure 8. Qualitative results on CIFAR-100. For each case, we illustrate the top-5 prediction for baseline network (upper) and with our attention supervision (bottom). The attention of target class is marked with red bounding box. Our model is able to correctly predict ‘sunflower’ and ‘leopard’, providing discriminative attention.

Method	Depth	Params	Acc.	Δ
ResNet-110 [14]	110	1.7M	72.78	-
ResNet with Stochastic Depth [14]	110	1.7M	75.42	-
ResNet (pre-activation) [11]	164	1.7M	75.63	-
ResNet-110 + \mathcal{A}_{px}	110	1.7M	76.24	3.46
ResNet-110 + \mathcal{A}_{ch}	110	1.7M	76.11	3.24

Table 2. Results of generic image classification on CIFAR-100. The last column Δ indicates performance improvement of the network with our attention-driven supervision when compared to the baseline model.

Method(N=30)	Top-1	Top-5	Δ
ResNet-18	76.77	92.48	-
ResNet-18 + \mathcal{A}_{px}	77.82	92.43	1.05
ResNet-18 + \mathcal{A}_{ch}	78.01	92.87	1.24
VGG-19	74.52	90.05	-
VGG-19 + \mathcal{A}_{px}	75.34	90.82	0.82
VGG-19 + \mathcal{A}_{ch}	75.60	90.85	1.08
Method (N=60)	Top-1	Top-5	Δ
ResNet-18	80.01	94.12	-
ResNet-18 + \mathcal{A}_{px}	81.34	94.20	1.33
ResNet-18 + \mathcal{A}_{ch}	81.32	94.57	1.31
VGG-19	78.16	92.17	-
VGG-19 + \mathcal{A}_{px}	79.53	93.22	1.37
VGG-19 + \mathcal{A}_{ch}	79.80	93.25	1.64

Table 3. Image classification results on Caltech-256 [10]. The last column Δ indicates performance improvement of the network with our attention-driven supervision when compared to the baseline model.

pipeline from [29] to choose ResNet-50 and ResNet-101 as the baseline models. The input images are resized to 448×448 for both training and testing and we apply

Method	Top-1	Top-5	Δ
ResNet-18 [11]	69.51	88.91	-
ResNet-18 + \mathcal{A}_{ch}	69.90	89.71	0.39
ResNet-18 + tenCrop [11]	72.12	90.58	-
ResNet-18 + tenCrop + \mathcal{A}_{ch}	73.04	90.65	0.92

Table 4. Image classification results on ILSVRC2012 [24]. The last column Δ indicates performance improvement of the network with our attention-driven supervision when compared to the baseline model.

Method	Anno.	1-Stage	Acc.
ResNet-50 [29]	✗	✓	81.7
ResNet-101 [29]	✗	✓	82.5
SPDA-CNN [36]	✓	✓	85.1
RACNN [9]	✗	✓	85.3
PN-CNN [3]	✓	✗	85.4
RAM [18]	✗	✗	86.0
MACNN + 2parts [38]	✗	✗	85.4
MACNN + 4parts [38]	✗	✗	86.5
ResNet-50 + MAMC [29]	✗	✗	86.2
ResNet-101 + MAMC [29]	✗	✗	86.5
ResNet-50 + \mathcal{A}_{ch}	✗	✓	86.2
ResNet-101 + \mathcal{A}_{ch}	✗	✓	86.5

Table 5. Results of fine-grained image classification on CUB-200-2011 [30].

standard augmentation for training data, *i.e.* mirror and random cropping. The SGD [2] is used to optimize the networks with a batch size of 10, initial learning rate of 0.001 (decayed by 0.1 after 30 and 60 epochs), for a total of 90 epochs.

The results on the CUB-200-2011 dataset are shown in Table 5. It is observed training with our learning mechanism boosts the performance of the baseline ResNet-50 and ResNet-101 by notable margins of 4.8% and 4.0% respectively. Our method achieves the best overall performance against state-of-the-art. With ResNet-50, our method exceeds the method using extra annotation (PN-CNN) by 0.8%.

Note that our approach has better flexibility compared to those methods in table 5. The existing approaches are specifically designed for fine-grained image recognition where, according the prior knowledge of the fine-grained species, the base architectures are modified to extract features of different objects parts [29, 36, 38]. Our approach does not need any prior knowledge and work for generic image classification without changing the network architecture.

Method	AUC Score	AP (%)	Δ (%)
ResNet-18	0.976	77.44	-
ResNet-34 [1]	-	80.7	-
ResNet-18 + \mathcal{A}_{px}	0.980	83.22	5.78
ResNet-18 + \mathcal{A}_{ch}	0.981	83.17	5.73

Table 6. Image classification results on PASCAL VOC 2012 [8]. The last column Δ indicates performance improvement of the network with our attention-driven supervision when compared to the baseline model.

4.3. Multi-class Image Classification

We conduct multi-class image classification on the PASCAL VOC 2012 dataset, which contains 20 classes. Different from the above generic and fine-grained image classification where each image is associated to one class label, for each of the twenty classes, the model predicts the probability of presence of an instance of that class in the test image. As our attention is class-specific, we can seamlessly adapt our pipeline from single-label to multi-label classification. In our experiments, we generate the class-concurrence attention maps by modifying the gradient computation. If there are multiple classes in one image, one-hot encoding is applied to corresponding dimensions in the predicted score vector.

We use ResNet-18 with the Multi-Label-Soft-Margin loss as our baseline model. To optimize the model, we use the same training recipe as in Caltech-256, where the weight decay is 0.001 with a momentum of 0.9 and initial learning rate of 0.01. Cyclic cosine annealing [13] with cycle of one is used to speed up the model training with 20 epochs.

Different from single label classification, we use the AUC score and Average Precision(AP) as the evaluation metric. We compute the AUC score via scikit-learn python module [23] and the AP is reported by the PASCAL evaluation server [8]. According to Table 6, the performance of ResNet-18 with the pixel and channel-wise attention supervision exceeds the baseline by the margin of 5.8% and 5.73% respectively. Furthermore, attention also helps ResNet-18 (18 feature layers) outperform the deeper model ResNet-34 (34 feature layers) in terms of average precision.

5. Conclusion

We proposed a trainable category discriminative attention mechanism to guide model training for image classification. Our proposed framework has better attention consistency among different layers than Grad-CAM [25], and is flexible to be added to any trainable network without changing network architectures, giving an end-to-end procedure to reduce model visual confusion. We show performance improvements on various medium-scale, large-scale, fine-grained and multi-class classification tasks.

References

- [1] Voc2012 classification results leaderboard. <http://host.robots.ox.ac.uk:8080/leaderboard/displaylb.php?challengeid=11&compid=1>.
- [2] L. Bottou. Large-scale machine learning with stochastic gradient descent. In *Proceedings of COMPSTAT'2010*, pages 177–186. Springer, 2010.
- [3] S. Branson, G. Van Horn, S. Belongie, and P. Perona. Bird species categorization using pose normalized deep convolutional nets. In *British Machine Vision Conference*, 2014.
- [4] A. Chattopadhyay, A. Sarkar, P. Howlader, and V. N. Balasubramanian. Grad-CAM++: Generalized gradient-based visual explanations for deep convolutional networks. In *2018 IEEE Winter Conference on Applications of Computer Vision (WACV)*, pages 839–847. IEEE, 2018.
- [5] A. Chaudhry, P. K. Dokania, and P. H. Torr. Discovering class-specific pixels for weakly-supervised semantic segmentation. *BMVC*, 2017.
- [6] A. Dosovitskiy and T. Brox. Inverting visual representations with convolutional networks. In *Proceedings of the IEEE Conference on Computer Vision and Pattern Recognition*, pages 4829–4837, 2016.
- [7] D. Erhan, Y. Bengio, A. Courville, and P. Vincent. Visualizing higher-layer features of a deep network. *University of Montreal*, 1341(3):1, 2009.
- [8] M. Everingham, L. Van Gool, C. K. I. Williams, J. Winn, and A. Zisserman. The PASCAL Visual Object Classes Challenge 2012 (VOC2012) Results. <http://www.pascal-network.org/challenges/VOC/voc2012/workshop/index.html>.
- [9] J. Fu, H. Zheng, and T. Mei. Look closer to see better: Recurrent attention convolutional neural network for fine-grained image recognition. In *CVPR*, volume 2, page 3, 2017.
- [10] G. Griffin, A. Holub, and P. Perona. Caltech-256 object category dataset. 2007.
- [11] K. He, X. Zhang, S. Ren, and J. Sun. Deep residual learning for image recognition. In *Proceedings of the IEEE conference on computer vision and pattern recognition*, pages 770–778, 2016.
- [12] J. Hu, L. Shen, and G. Sun. Squeeze-and-excitation networks. In *Proceedings of the IEEE Conference on Computer Vision and Pattern Recognition*, pages 7132–7141, 2018.
- [13] G. Huang, Y. Li, G. Pleiss, Z. Liu, J. E. Hopcroft, and K. Q. Weinberger. Snapshot ensembles: Train 1, get m for free. *ICLR*, 2017.
- [14] G. Huang, Y. Sun, Z. Liu, D. Sedra, and K. Q. Weinberger. Deep networks with stochastic depth. In *European Conference on Computer Vision*, pages 646–661. Springer, 2016.
- [15] S. Jetley, N. A. Lord, N. Lee, and P. H. Torr. Learn to pay attention. In *International Conference on Learning Representations*, 2018.
- [16] A. Krizhevsky and G. Hinton. Learning multiple layers of features from tiny images. Technical report, Citeseer, 2009.
- [17] K. Li, Z. Wu, K.-C. Peng, J. Ernst, and Y. Fu. Tell me where to look: Guided attention inference network. *CVPR*, 2018.
- [18] Z. Li, Y. Yang, X. Liu, F. Zhou, S. Wen, and W. Xu. Dynamic computational time for visual attention. In *ICCV*, 2017.
- [19] A. Mahendran and A. Vedaldi. Understanding deep image representations by inverting them. In *Proceedings of the IEEE conference on computer vision and pattern recognition*, pages 5188–5196, 2015.
- [20] A. Newell, K. Yang, and J. Deng. Stacked hourglass networks for human pose estimation. In *European Conference on Computer Vision*, pages 483–499. Springer, 2016.
- [21] J. Park, S. Woo, J.-Y. Lee, and I. S. Kweon. BAM: bottleneck attention module. *arXiv preprint arXiv:1807.06514*, 2018.
- [22] A. Paszke, S. Gross, S. Chintala, G. Chanan, E. Yang, Z. DeVito, Z. Lin, A. Desmaison, L. Antiga, and A. Lerer. Automatic differentiation in pytorch. In *NIPS-W*, 2017.
- [23] F. Pedregosa, G. Varoquaux, A. Gramfort, V. Michel, B. Thirion, O. Grisel, M. Blondel, P. Prettenhofer, R. Weiss, V. Dubourg, J. Vanderplas, A. Passos, D. Cournapeau, M. Brucher, M. Perrot, and E. Duchesnay. Scikit-learn: Machine learning in Python. *Journal of Machine Learning Research*, 12:2825–2830, 2011.
- [24] O. Russakovsky, J. Deng, H. Su, J. Krause, S. Satheesh, S. Ma, Z. Huang, A. Karpathy, A. Khosla, M. Bernstein, A. C. Berg, and L. Fei-Fei. ImageNet Large Scale Visual Recognition Challenge. *International Journal of Computer Vision (IJCV)*, 115(3):211–252, 2015.
- [25] R. R. Selvaraju, M. Cogswell, A. Das, R. Vedantam, D. Parikh, D. Batra, et al. Grad-CAM: Visual explanations from deep networks via gradient-based localization. In *ICCV*, pages 618–626, 2017.
- [26] K. Simonyan, A. Vedaldi, and A. Zisserman. Deep inside convolutional networks: Visualising image classification models and saliency maps. In *International Conference on Learning Representations Workshop*, 2014.
- [27] K. Simonyan and A. Zisserman. Very deep convolutional networks for large-scale image recognition. *arXiv preprint arXiv:1409.1556*, 2014.
- [28] J. T. Springenberg, A. Dosovitskiy, T. Brox, and M. Riedmiller. Striving for simplicity: The all convolutional net. In *International Conference on Learning Representations Workshop*, 2015.
- [29] M. Sun, Y. Yuan, F. Zhou, and E. Ding. Multi-attention multi-class constraint for fine-grained image recognition. In *ECCV*, 2018.
- [30] C. Wah, S. Branson, P. Welinder, P. Perona, and S. Belongie. The Caltech-UCSD Birds-200-2011 Dataset. Technical Report CNS-TR-2011-001, California Institute of Technology, 2011.
- [31] C. Wah, S. Branson, P. Welinder, P. Perona, and S. Belongie. The Caltech-UCSD Birds-200-2011 Dataset. Technical Report CNS-TR-2011-001, California Institute of Technology, 2011.
- [32] F. Wang, M. Jiang, C. Qian, S. Yang, C. Li, H. Zhang, X. Wang, and X. Tang. Residual attention network for image classification. In *Proceedings of the IEEE Conference on Computer Vision and Pattern Recognition*, pages 3156–3164, 2017.
- [33] Y. Wei, J. Feng, X. Liang, M.-M. Cheng, Y. Zhao, and S. Yan. Object region mining with adversarial erasing: A simple classification to semantic segmentation approach. In *IEEE CVPR*, volume 1, page 3, 2017.
- [34] S. Woo, J. Park, J.-Y. Lee, and I. S. Kweon. CBAM: Convolutional block attention module. In *Proc. of European Conf.*

- on *Computer Vision (ECCV)*, 2018.
- [35] M. D. Zeiler and R. Fergus. Visualizing and understanding convolutional networks. In *European conference on computer vision*, pages 818–833. Springer, 2014.
 - [36] H. Zhang, T. Xu, M. Elhoseiny, X. Huang, S. Zhang, A. Elgammal, and D. Metaxas. Spda-cnn: Unifying semantic part detection and abstraction for fine-grained recognition. In *Proceedings of the IEEE Conference on Computer Vision and Pattern Recognition*, pages 1143–1152, 2016.
 - [37] X. Zhang, Y. Wei, J. Feng, Y. Yang, and T. Huang. Adversarial complementary learning for weakly supervised object localization. In *IEEE CVPR*, 2018.
 - [38] H. Zheng, J. Fu, T. Mei, and J. Luo. Learning multi-attention convolutional neural network for fine-grained image recognition. In *Int. Conf. on Computer Vision*, volume 6, 2017.
 - [39] B. Zhou, A. Khosla, A. Lapedriza, A. Oliva, and A. Torralba. Learning deep features for discriminative localization. In *Proceedings of the IEEE Conference on Computer Vision and Pattern Recognition*, pages 2921–2929, 2016.